

Half-cycle atomic layer deposition reaction studies of Al_2O_3 on $\text{In}_{0.2}\text{Ga}_{0.8}\text{As}$ (100) surfaces

M. Milojevic, F. S. Aguirre-Tostado, C. L. Hinkle, H. C. Kim, E. M. Vogel, J. Kim, and R. M. Wallace

Citation: *Appl. Phys. Lett.* **93**, 202902 (2008); doi: 10.1063/1.3033404

View online: <http://dx.doi.org/10.1063/1.3033404>

View Table of Contents: <http://aip.scitation.org/toc/apl/93/20>

Published by the [American Institute of Physics](#)

 **Lake Shore**
CRYOTRONICS



NEW 8600 Series VSM

For fast, highly sensitive
measurement performance

LEARN MORE 

Half-cycle atomic layer deposition reaction studies of Al₂O₃ on In_{0.2}Ga_{0.8}As (100) surfaces

M. Milojevic, F. S. Aguirre-Tostado, C. L. Hinkle, H. C. Kim, E. M. Vogel, J. Kim,^{a)} and R. M. Wallace^{b)}

Department of Materials Science and Engineering, University of Texas at Dallas, Richardson, Texas 75083, USA

(Received 16 June 2008; accepted 29 October 2008; published online 19 November 2008)

The reduction in III–V interfacial oxides by atomic layer deposition of Al₂O₃ on InGaAs is studied by interrupting the deposition following individual trimethyl aluminum (TMA) and water steps (half cycles) and interrogation of the resultant surface reactions using *in situ* monochromatic x-ray photoelectron spectroscopy (XPS). TMA is found to reduce the interfacial oxides during the *initial* exposure. Concentrations of Ga oxide on the surface processed at 300 °C are reduced to a concentration on the order of a monolayer, while AsO_x species are below the level of detection of XPS. © 2008 American Institute of Physics. [DOI: 10.1063/1.3033404]

Engineering the chemistry at the substrate/dielectric interface is critical to the manufacturing of a high performance metal-oxide-semiconductor (MOS) device on III–V substrates.^{1–3} Controlling the oxidation state and the relative amount of Ga–O and As–O have been shown recently to be directly related to the accumulation capacitance frequency dispersion phenomenon.⁴ A Si-interfacial passivation layer (IPL) can be used to control surface oxidation,^{5–8} although it is currently unclear if this compromises some of the performance potential of the MOS device.^{9,10} Ideally the dielectric deposition process itself, combined with appropriate surface preparation, might remove the need for an IPL. In a previous atomic layer deposition (ALD) study, it has been reported that both precursor and oxidation state dependent reactions effect interfacial oxide formation on GaAs.¹¹ This “clean-up” effect indicates that the interfacial bonding type can be controlled by varying the deposition conditions, as seen in previous *ex situ* studies on GaAs.^{12–14} Previous *ex situ* analysis of the InGaAs interface has reported similar clean-up effects for HfO₂ deposited by ALD.¹⁵ In this work, we examine the ALD dielectric deposition process in detail by interrupting the growth cycle (referred to here as “half cycles” of the ALD process) with *in situ* monochromatic x-ray photoelectron spectroscopy (XPS) analysis to characterize the surface reactions associated with the ALD of trimethyl aluminum (TMA) on In_{0.2}Ga_{0.8}As.

The samples used in this study were *n*-type (Si, $1 \times 10^{18}/\text{cm}^3$) epitaxial¹⁶ In_{0.2}Ga_{0.8}As. The In_{0.2}Ga_{0.8}As structure was grown by starting with a semi-insulating GaAs substrate on top of which a 150 nm buffer layer of *n*-GaAs (Si, $4 \times 10^{17}/\text{cm}^3$) followed by growth of a 130 nm layer of *n*-GaAs (Si, $1 \times 10^{17}/\text{cm}^3$). Finally a 13.5 nm thick active layer of In_{0.2}Ga_{0.8}As was grown with a 1:4 In to Ga ratio confirmed by XPS.

Samples were initially degreased for 1 min in each of acetone, methanol, and isopropyl alcohol. The native oxides were etched using HCl:de-ionized water (DIW) (1:1) for 10 min followed by a rinse in flowing DIW for <10 s. The final treatment involved a 10 min dip in (NH₄)₂S (22%)

and a DIW rinse.¹⁷ Samples were then mounted and introduced into an ultrahigh vacuum (UHV) system in less than 10 min. A dual chamber ALD reactor¹⁸ integrated to an UHV multitechnique deposition/characterization system was used for this *in situ* study.¹⁹ TMA was used as the Al precursor for subsequent Al₂O₃ formation using water deposition chemistry. Prior to the first ALD deposition, the unloaded reactor was baked at 400 °C and exposed to 300 cycles [1 cycle=0.1 s (TMA/N₂)+4 s N₂+0.1 s (H₂O/N₂)+4 s N₂] in order to encourage reproducible reaction behavior and reduce any spurious wall deposition/reaction effects due to residual precursor components from previous depositions.²⁰ High purity (99.999%) N₂ is used as the purging gas. Two separate sets of film depositions were performed at sample/reactor temperatures of 200 and 300 °C. The ALD chamber pressure was ~7.6 Torr during deposition, and was connected to the sample analysis module through a UHV transport tube by a buffer chamber. The pressure of the UHV transport tube during wafer transfer between half-cycles was $<2 \times 10^{-10}$ mbar, enabling surface characterization without spurious *ex situ* atmospheric exposure or contamination from the vacuum as determined by control experiments (not shown). Analysis of the deposited films was done using an *in situ* monochromatic XPS using an Al K α x-ray source (1486.7eV) (Ref. 21) with a linewidth of ~0.25 eV and pass energy of 15 eV.²² XPS data were taken following each half cycle (TMA/N₂+XPS, then H₂O/N₂+XPS). The take-off angle from the substrate surface was 45°, with an analyzer acceptance angle of 16°. Binding energy calibration is performed regularly to accepted procedures.²³

Figure 1(a) shows the Al 2*p* feature, which indicates fully oxidized Al after each TMA pulse, and is consistent with the O 1*s* peak in Fig. 1(b), which compares the O 1*s* peak before and after the first TMA pulse at 300 °C. The primary components prior to TMA exposure are attributed to As–O, Ga–O, and In–O bonding.^{24,25} Importantly, the total O 1*s* peak intensity does not change following the first TMA pulse, indicating that the Al is oxidized at the expense of the interfacial substrate oxides. Both remaining Ga–O and In–O bonding features are reduced in intensity and appear at a lower binding energy (~530.8 eV) than Al–O bonds (~531.3 eV).²⁶ Therefore as these surface oxides are re-

^{a)}Electronic mail: jiyoun.kim@utdallas.edu.

^{b)}Electronic mail: rmwallace@utdallas.edu.

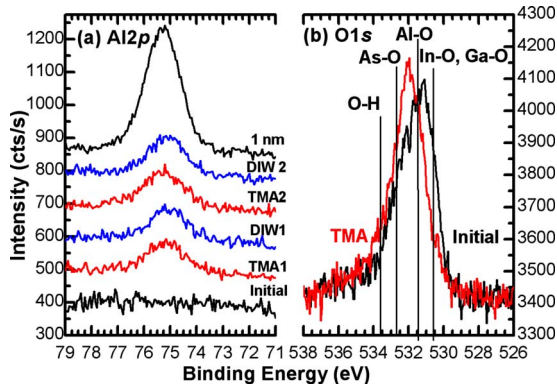


FIG. 1. (Color online) (a) Al $2p$ region following the first (TMA1, DIW1) and second (TMA2, DIW2) half-cycle exposures as well as after ten full cycles (1 nm) at 300 °C on $\text{In}_{0.2}\text{Ga}_{0.8}\text{As}$. (b) O $1s$ peak before and after the first TMA pulse showing a shift toward a higher binding energy but no change in total area.

duced and Al–O bond formation ensues, the O $1s$ peak appears to shift to higher binding energy, with possible Al–OH bond formation as well.²⁷ The C $1s$ intensity (not shown) is near the limit of detection and appears unaffected by the subsequent ALD cycles, suggesting that the C incorporated originates with the TMA precursor.

Figure 2 shows the Ga $2p_{3/2}$ peak following surface preparation, after the first TMA pulse, and further after a 1 nm thick Al_2O_3 film (ten full cycles) is grown. We note that the surfaces prepared for the subsequent 200 °C ALD experiments have slightly higher initial oxide content at the surface and are attributed to surface preparation variations. The higher binding energy peak (~ 1118.4 eV) corresponds

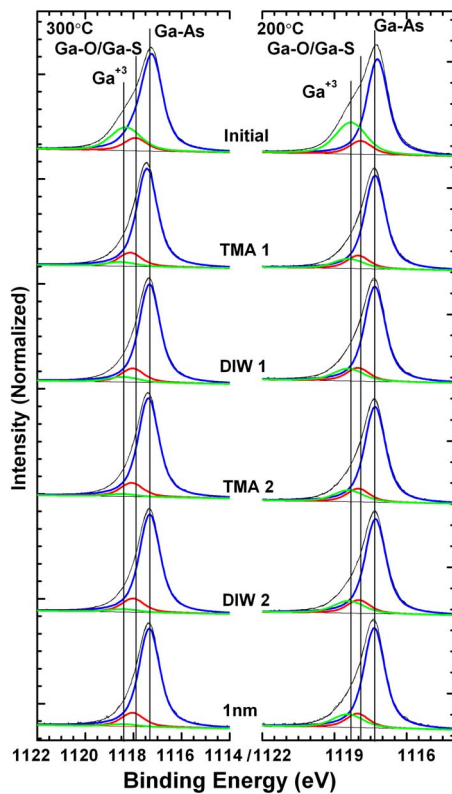


FIG. 2. (Color online) Ga $2p_{3/2}$ spectra showing the reduction in gallium oxides following the first four half cycles and the subsequent spectra upon completion of the 1 nm ALD Al_2O_3 film at 200 and 300 °C.

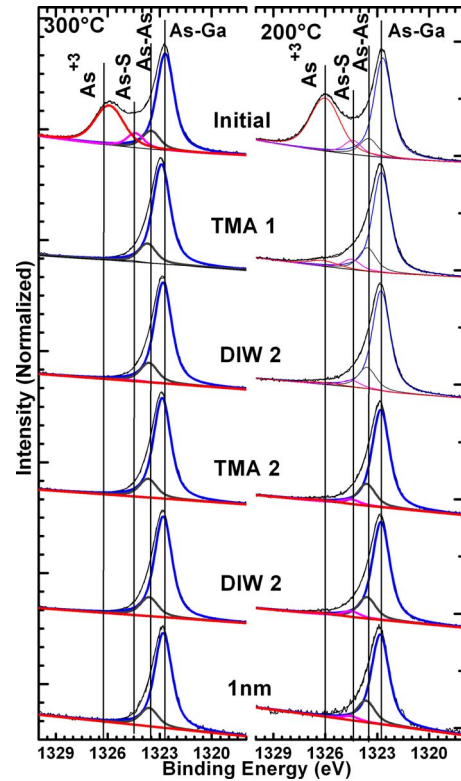


FIG. 3. (Color online) As $2p_{3/2}$ spectra showing the removal of arsenic oxides following the first four half cycles and the subsequent spectra upon completion of the 1 nm ALD Al_2O_3 film at 200 and 300 °C.

to Ga^{3+} bonding while the bulk Ga–As bonding is contained in the primary peak at (~ 1117.3 eV). The position of the Ga–O suboxide peak (~ 1117.9 eV) has been derived by Hinkle *et al.*²⁸ from detailed photoelectron studies.^{29–31} A peak corresponding to a Ga–S bond is difficult to resolve from this suboxide peak.³² After the first TMA exposure, the Ga^{3+} oxidation state is dramatically reduced for both deposition temperatures. This indicates that the *initial* metal precursor TMA pulse is primarily responsible for the clean up of interfacial oxides. The area ratio of residual gallium oxides to the Ga–As is found to be 0.15, which is calculated by taking into account the escape depth of a 360 eV electron to correspond to signal on the order of a monolayer.

We also compare the As $2p_{3/2}$ features (Fig. 3), where the surface-sensitive high binding energy peak is attributed to an As^{3+} oxidation state (~ 1326 eV), As–S bonding³³ (~ 1324.5 eV), and As–As bonding (~ 1323.5 eV).^{24,32} The first TMA pulse is effective at reducing arsenic oxide and sulfide bonding below the level of detection of XPS at 300 °C but not at 200 °C. This behavior likely stems from the relatively weak bonding³⁴ and as well as the relatively high vapor pressure of elemental As.³⁵ Since the native oxides of III–V compounds may be thought of as a glassy network connected by oxygen atoms,³⁰ increasing the temperature from 200 to 300 °C would aid in destabilizing the entire structure, even though As–O bond scission dominates at such deposition temperatures.

The tendency of reducing agents such TMA to preferentially attack trivalent oxides is confirmed by the dramatic reduction in trivalent gallium and arsenic oxides and the constant Ga–O/Ga–As intensity ratio with growth. The In $3d$ peaks (not shown) show much lower levels of initial oxida-

tion than the Ga 2p spectra. It is reasonable to expect that the extent of interfacial oxide reduction depends on temperature as well as the surface concentration of reducing species (i.e., TMA). It has been shown that the surface concentration of adsorbed TMA is inversely proportional to the substrate temperature,³⁶ which would cause a diminished clean-up effect at higher substrate temperatures due to a lower surface concentration of TMA. We observe the opposite, however, which suggests that the kinetics of the reaction depend primarily on temperature.

In conclusion, the results show that for TMA/water based alumina ALD, the first TMA half cycle pulse is responsible for the interfacial oxide reduction. At 300 °C, As–O bonding is reduced below the XPS level of detection and Ga–O bonding is reduced to the order of monolayer concentration at the interface demonstrating a sharp substrate/oxide interface. Similar measurements of the ALD reactions performed at 200 °C indicate that the clean-up effect was less effective.

The authors acknowledge the useful discussions with Dr. M. Passlack. This work is supported by the FCRP on Materials, Structures, and Devices, the National Institute of Standards and Technology, Semiconductor Electronics Division, System IC 2010 (funded by MKE in Korea), and the Texas Enterprise Fund.

¹T. Ito and Y. Sakai, *Solid-State Electron.* **17**, 751 (1974).

²M. Passlack, in *Materials Fundamentals of Gate Dielectrics*, edited by A. A. Demkov and A. Navrotsky (Springer, Berlin, 2005), pp. 403–467.

³M. Hong, J. R. Kwo, P. Tsai, Y. Chang, M. Huang, C. Chen, and T. Lin, *Jpn. J. Appl. Phys., Part 1* **46**, 3167 (2007).

⁴C. L. Hinkle, A. M. Sonnet, E. M. Vogel, S. McDonnell, G. J. Hughes, M. Milojevic, B. Lee, F. S. Aguirre-Tostado, K. J. Choi, J. Kim, and R. M. Wallace, *Appl. Phys. Lett.* **91**, 163512 (2007).

⁵S. Tiwari, S. L. Wright, and J. Batey, *IEEE Electron Device Lett.* **9**, 488 (1988).

⁶J. L. Freeouf, D. A. Buchanan, S. L. Wright, T. N. Jackson, J. Batey, B. Robinson, A. Callegari, A. Paccagnella, and J. M. Woodall, *J. Vac. Sci. Technol. B* **8**, 860 (1990); J. L. Freeouf, D. A. Buchanan, S. L. Wright, T. N. Jackson, and B. Robinson, *Appl. Phys. Lett.* **57**, 1919 (1990).

⁷J. Ivanco, T. Kubota, and H. Kobayashi, *J. Appl. Phys.* **97**, 073712 (2005).

⁸S. Koveshnikov, W. Tsai, I. Ok, J. C. Lee, V. Tokranov, M. Yakimov, and S. Oktyabrsky, *Appl. Phys. Lett.* **88**, 022106 (2006).

⁹D. J. Webb, J. Fompeyrine, S. Nakagawa, A. Dimoulas, C. Rossel, M. Sousa, R. Germann, S. F. Alvarado, J. P. Locquet, C. Marchiori, H. Siegwart, A. Callegari, E. Kiewra, Y. Sun, J. De Souza, and N. Hoffmann, *Microelectron. Eng.* **84**, 2142 (2007).

¹⁰J. P. de Souza, E. Kiewra, Y. Sun, A. Callegari, D. K. Sadana, G. Shahidi, D. J. Webb, J. Fompeyrine, R. Germann, C. Rossel, and C. Marchiori, *Appl. Phys. Lett.* **92**, 153508 (2008).

¹¹C. L. Hinkle, A. M. Sonnet, E. M. Vogel, S. McDonnell, G. J. Hughes, M. Milojevic, B. Lee, F. S. Aguirre-Tostado, K. J. Choi, H. C. Kim, J. Kim, and R. M. Wallace, *Appl. Phys. Lett.* **92**, 071901 (2008).

¹²P. D. Ye, G. D. Wilk, B. Yang, J. Kwo, S. N. G. Chu, S. Nakahara, H.-J. L. Gossmann, J. P. Mannaerts, M. Hong, K. K. Ng, and J. Bude, *Appl. Phys. Lett.* **83**, 180 (2003).

¹³M. L. Huang, Y. C. Chang, C. H. Chang, Y. J. Lee, P. Chang, J. Kwo, T. B. Wu, and M. Hong, *Appl. Phys. Lett.* **87**, 252104 (2005).

¹⁴M. M. Frank, G. D. Wilk, D. Starodub, T. Gustafsson, E. Garfunkel, Y. J. Chabal, J. Grazul, and D. A. Muller, *Appl. Phys. Lett.* **86**, 152904 (2005).

¹⁵C. H. Chang, Y. K. Chiou, Y. C. Chang, K. Y. Lee, T. D. Lin, T. B. Wu, M. Hong, and J. Kwo, *Appl. Phys. Lett.* **89**, 242911 (2006).

¹⁶Intelligent Epitaxy Technologies, <http://www.intelliepi.com>.

¹⁷M. H. Zhang, M. Oye, B. Cobb, F. Zhu, H. S. Kim, I. J. Ok, J. Hurst, S. Lewis, A. Holmes, J. C. Lee, S. Koveshnikov, W. Tsai, M. Yakimov, V. Tokranov, and S. Oktyabrsky, *J. Appl. Phys.* **101**, 034103 (2007).

¹⁸Picosun Oy (<http://www.picosun.com>).

¹⁹P. Sivasubramani, J. Kim, M. J. Kim, B. E. Gnade, and R. M. Wallace, *J. Appl. Phys.* **101**, 114108 (2007).

²⁰The TMA pulse partial pressure is 300 mbar.

²¹J. Schweppe, R. D. Deslattes, T. Mooney, and C. J. Powell, *J. Electron Spectrosc. Relat. Phenom.* **67**, 463 (1994).

²²Omicron Nanotechnology, GmbH (<http://www.omicron.de>).

²³Standard practice for calibration of the electron binding-energy scale of an x-ray photoelectron spectrometer," ASTM Standard Report No. E2108-05, ASTM International, West Conshohocken, PA, www.astm.org; C. J. Powell, *Surf. Interface Anal.* **23**, 121 (1995); M. P. Seah, I. S. Gilmore, and G. Beamson, *ibid.* **26**, 642 (1998).

²⁴M. V. Lebedev, D. Enslin, R. Hunger, T. Mayer, and W. Jaegermann, *Appl. Surf. Sci.* **229**, 226 (2004).

²⁵F. S. Aguirre-Tostado, M. Milojevic, C. L. Hinkle, E. M. Vogel, R. M. Wallace, S. McDonnell, and G. J. Hughes, *Appl. Phys. Lett.* **92**, 171906 (2008).

²⁶J. F. Moulder, W. F. Stickle, P. E. Sobol, and K. D. Bomben, *Handbook of X-ray Photoelectron Spectroscopy* (Physical Electronics, Eden Prairie, MN, 1995), pp. 230–232.

²⁷B. R. Strohmeier, *J. Vac. Sci. Technol. A* **7**, 3238 (1989).

²⁸C. L. Hinkle, M. Milojevic, B. Brennan, A. M. Sonnet, F. S. Aguirre-Tostado, G. J. Hughes, E. M. Vogel, and R. M. Wallace, "Detection of Ga suboxides and their impact on III-V passivation and Fermi-level pinning" (unpublished).

²⁹G. Landgren, R. Ludeke, J. F. Morar, Y. Jugnet, and F. J. Himpsel, *Phys. Rev. B* **30**, 4839 (1984).

³⁰G. Hollinger, R. Skheyta-Kabbani, and M. Gendry, *Phys. Rev. B* **49**, 11159 (1994).

³¹J. Ivanco, T. Kubota, and H. Kobayashi, *J. Appl. Phys.* **97**, 073712 (2005).

³²S. Arabasz, E. Bergignat, G. Hollinger, and J. Szuber, *Appl. Surf. Sci.* **252**, 7659 (2006).

³³Z. H. Lu, M. J. Graham, X. H. Feng, and B. X. Yang, *Appl. Phys. Lett.* **62**, 2932 (1993).

³⁴For example, As₂O₃ melting point ~313 °C cf. Ga₂O₃ melting point >1725 °C; see <http://www.webelements.com/>.

³⁵C. Sasaoka, Y. Kato, and A. Usui, *Appl. Phys. Lett.* **62**, 2338 (1993).

³⁶R. L. Puurunen, *J. Appl. Phys.* **97**, 121301 (2005).